

ROSPA, CROSS-VALIDATION OF THE PLATFORM-ART AND ORBIT TEST FACILITIES FOR CONTACT DYNAMIC SCENARIO SETUP AND STUDY

*Andrea Pellacani**, *Hendrik Kolvenbach***

*GMV, Spain, apellacani@gmail.com

** ESTEC, The Netherlands, hendrik.kolvenbach@esa.int

ABSTRACT

The set-up and use of ground validation testing facilities from the early phases of the missions can provide a very valuable feedback to the equipment and technologies being developed. The validation activities of the ground testing facilities are key to the usability and confidence of the results obtained from them. GMV's *platform-art* dynamic test bench has already been validated (for navigation purposes based on optical cameras) with flight data coming from PRISMA mission through the PRISMA-HARVD experiment. In addition, *platform-art* dynamic test bench is currently being extended thanks to ESA loan of several new devices, including a new high-span KUKA robotic arm, which will extend the functionality of the current test bench. On the other hand, ESA has established an air-bearing facility known as ORBIT (Orbit Robotics Bench for Integrated Technology). The facility located within ESTEC's Automation and Robotic laboratories provides several air-bearing platforms which can move frictionless on a 45 m² flat floor.

The in-space Robotic Servicing Physical Assessment (ROSPA) is a study with the purpose of recreating and studying the dynamics during/after contact between target and chaser in a rendezvous and capture mission. The data of the experiments run in the *platform-art* (GMV) and in ORBIT (ESA) will be used for a cross-validation of the facilities.

Two different scenarios have been setup in both facilities: simple contact and gripping scenario. In the simple contact scenario a Mitsubishi PA10 robotic arm approaches the specifically designed mock-up mounted on the air-bearing (or on a KUKA robotic arm, in *platform-art*) and touches it through a compliance device and a load cell to measure the contact forces and torques. In the gripping scenario the compliance device is replaced by a gripping device, which after an open loop trajectory attempts the gripping of a Launch Adapter Ring (LAR) mock-up.

In the scope of the activity also another functionality of the *platform-art* facility is exploited: the space-like environment simulation. This functionality has been developed and demonstrated in the frames of previous collaborations between ESA and GMV, for projects such as NEOGNC (Interplanetary mission, MarcoPolo-R) and

ANDROID (Active Debris removal mission). The output of this activity is a data base of representative images taken during an open loop sequence of the robotic arm approach and the gripping with the LAR of a mock-up of the TANGO spacecraft (the 2nd spacecraft of the Swedish PRISMA mission). The representativeness of the images in such a close range scenario is meant in terms of illumination conditions and disturbances recreated in laboratory like fuel on lens, micro pieces of MLI floating and thruster plume in the Camera FoV.

1. INTRODUCTION

The purpose of the ROSPA activity is to cross-validate the ORBIT [1] and the *platform-art* [2] facilities as far as contact dynamic reproduction and investigation is concerned. The selected scenarios, the laboratory set-up and the devices adopted for this purpose are reported in the paper to have a full comprehension of the results and of the boundaries conditions under which the drawn conclusion are valid. In the scope of the activity also a database of representative images of a debris removal scenario is generated, recreating several types of disturbances and effects that may occur in such a scenario.

The tests are subdivided into two main groups. The 3 Degree of Freedom tests (3 DOF) which were used for the cross-validation of the facilities and the 6 Degree of Freedom tests (6 DOF), performed only at *platform-art*, to generate the image database.

2. SCENARIOS DEFINITION

2.1. 3 DOF test scenario

The 3DOF test scenario was conducted at the ORBIT and *platform-art* facility.

The purpose of these tests is to evaluate the dynamic evolution during/after the contact between a chaser and a target satellite.

The test scenario at the ORBIT facility considered the Mitsubishi PA10 robotic arm as the chaser and a mock-up mounted on an air-bearing platform as target. In the *platform-art* test facility the target mock-up was mounted on the KUKA robotic arm which substituted the air-bearing platforms.

The nominal relative trajectory between target and chaser is the output of the scenario simulator developed at GMV using the *Spacelab* libraries of GNCDE¹. This trajectory was tested at the ORBIT test facility and the obtained telemetry defined the reference trajectory to be adopted in *platform-art*. This scheme was selected since the air-bearing platform in the ORBIT test facility cannot be controlled with sub-millimeter precision which would be necessary for accurately reproducing the simulated (nominal) scenario. However, it was possible to obtain its pose during the tests with sub-millimeter precision. Thus, the air-bearing platform telemetry was adopted as the reference scenario.

It is important to remark that the contact forces and torques recorded in the experiment in the ORBIT facility are not simulated, but they are the real ones, occurred during an impact of a real contact scenario.

Next, the reference scenario was recreated in the *platform-art* test bench (with sub-millimeter control capability). The cross-validation strategy is resumed in Figure 1.

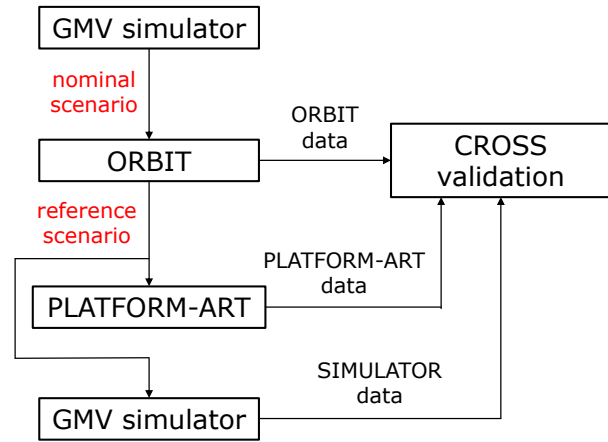


Figure 1: Scheme of the cross-validation strategy

The GMV simulator contains two simple contact models. A one and two-dimensional contact model has been developed. Considering the selected scenario, the one-dimensional model has been selected. The adopted spring/damper equations are reported below:

$$\dot{x} = V$$

$$m\dot{V} = F$$

¹ The Guidance Navigation and Control Development Environment (GNCDE) is a tool developed during a collaboration between ESA and GMV for the design, simulation and validation of GNC algorithms.

$$F = \begin{cases} -c(V - V_c) - k(|x - x_c| - s) \frac{x - x_c}{|x - x_c|}, & \forall F \cdot \frac{x - x_c}{|x - x_c|} \geq 0 \text{ and } |x - x_c| \leq s \\ 0, & \forall F \cdot \frac{x - x_c}{|x - x_c|} < 0 \text{ or } |x - x_c| > s \end{cases}$$

Where x and V are the position and velocity of the mock-up center of mass, x_c and V_c are the same but for the base of the compliance device, c the coefficient of damping, k the stiffness coefficient, m the mass of the air-bearing platform and s the distance between the mock-up center of mass and the base of the compliance device to have the spring in its natural elongation.

Figure 2 and Figure 3 show a schematic view of the experiment execution at ORBIT. For reasons of clarity, the XY and YZ plane views are reported (the reference system is the Fixed Reference Frame, fixed to the base of the PA10). A linear movement of the PA10 is considered. A point contact was selected as the contact scenario between chaser and target. This is realized by having a spherical probe on the robotic arm and a cylindrical structure as the mock-up mounted on the air-bearing (in the figures Mantis is taken as an example).

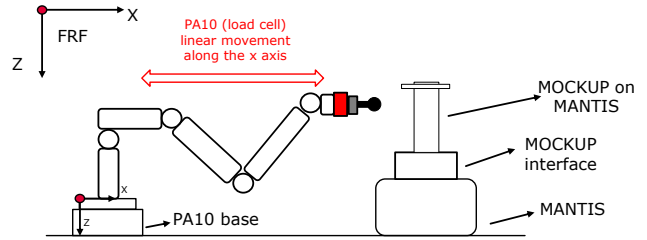


Figure 2: 3 DOF tests - XZ view

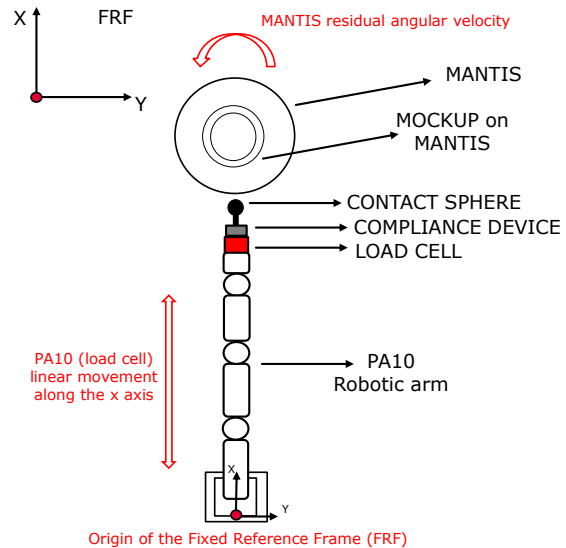


Figure 3: 3 DOF tests - XY view

Several approach velocity of the robotic arm have been tested and three different air-bearing platforms have been used.

2.2. 6 DOF tests scenario

The 6 DOF test scenario was performed only in *platform-art*. The purpose was to generate an image database with various sensor degradations which were taken during an open-loop gripping sequence of a TANGO satellite mock-up.

The device adopted to take pictures was a laboratory camera mounted near the base of the PA10 robotic arm (e.g. navigation camera role). A second camera, placed at the tip of the robotic arm has been used for gripping confirmation.

Closed-loop errors have been considered for the 6 DOF tests, resulting from the outputs of the COBRA-IRIDES activity². Here below the closed loop final performance are reported in terms of bias and random noise to add to the guidance trajectory and attitude profile. The data reported in Table 1 are meant to give an order of magnitude of the expected performance in an ADR scenario; the image processing algorithm, the geometry of the target and the accuracy of the sensors on the chaser strongly affect these performances. The errors reported in the table have been taken into account in the 6 DOF open loop trajectory.

Closed loop errors from behavioural models	Relative position errors [m]	Relative attitude errors [deg]
Bias: residual bias, misalignment and mounting errors.	0.005 m	0.01 deg
Random noise: statistic approximation	0.03 m (3-sigma value)	0.8 deg (3-sigma value)

Table 1: Closed loop errors in the 6 DOF

Figure 4 gives a schematic view of the scenarios and sensor degradations of the 6 DOF tests.

² The scope of the COBRA-IRIDES activity was the rendezvous and deorbiting using chemical propulsion (thruster plume) of a non-cooperative free drifting debris. In such a scenario, the navigation errors are the most relevant ones

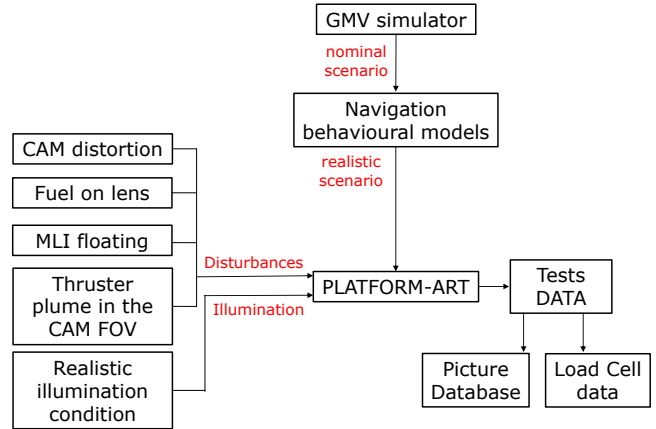


Figure 4: Scheme of the 6 DOF scenario

The approach trajectory consists of two parts. First, a residual relative angular motion of the mock-up is considered which simulates the synchronization of the chaser with the debris. Second, the robotic arm approaches the target and the gripping device grabs the LAR. Figure 5 gives an overview of the test setup in *platform-art*.

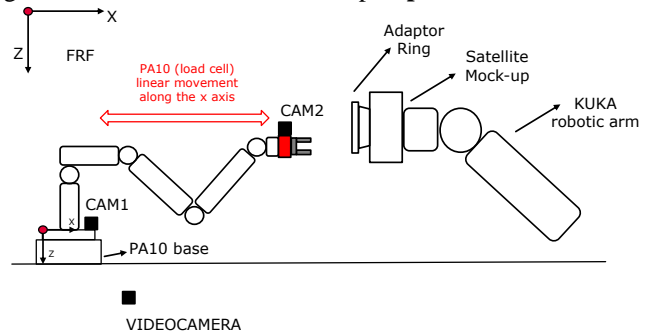


Figure 5: 6 DOF tests - XZ view

3. FACILITIES SET-UP

3.1. platform-art set up

The presence of heterogeneous HW (robotic arms from different manufacturers and illumination system) together with the need for executing a chain of hierarchical tasks, makes the selection of a distributed computing architecture necessary. The major elements are:

- The Motion Control System. It receives the kinematics information from the Real World simulator (DSpace host) through UDP messages and processes it by performing the following tasks:
 - Motion frames conversion
 - Motion solving for the different mechanical devices
 - Safety checks

- Send the motion solution to each of the specific control applications (of the robotic arms, track and illumination system) and trigger its execution in a synchronized way.

Also, the Motion Control System is the responsible of the Mitsubishi PA-10 robot and the illumination control system. These two applications have been physically placed in the same host machine for economy reasons but can be run in separated machines.

- The KUKA KR C2 controller system. It receives its motion solution from the Motion Control System and executes the motion command for the KUKA robotic arms and tracks motion system. It is also in charge of collecting the status and diagnostic information from KUKA devices on demand from the Motion Control System. It is connected through Ethernet to the Motion Control System due to the fact that it must physically travel on-board the track motion platform for constructive reasons.
- The net architecture selected is Ethernet at link level, IP at net level and UDP or TCP at transport level. Ethernet is a cheap and flexible solution already implemented for previous projects in the platform-art test facility
- The devices are interconnected through a switch. A switch is able to work at net level, what means that it is able to recognize IP directions and route the packets only through the switch port where the device with that IP address is located. It eliminates possible collisions with devices different from the target one.
- The communication logic at high level relies on the Motion Control System application that in practice acts as a master, sending execution orders and collecting information from the other applications.
- The Motion Control System process is triggered by the dSPACE host. The dSPACE host sends UDP datagrams through the Ethernet at a given frequency that contains the kinematics information to be reproduced. The Motion Control System processes each new datagram and sends the corresponding commands to the other application that traduces the movement order to the final motion devices.

3.2. ORBIT set up

Considering the nature of the experiment in the ORBIT test facility, the architecture of the test bench setup is similar but with less elements:

- The acquisition and control PC synchronizes the Vicon control PC for motion tracking and the Mitsubishi PA 10 robotic arm, in order to relate the robotic arm motion to the dynamic evolution of the air bearings.
- The Mitsubishi PA10 control PC executes the pre-defined open loop trajectory.
- The Vicon control PC is the responsible to collect and save real time the Vicon measurements in order to have the telemetry of the PA10 and of the motion of the air bearing platforms.

4. HARDWARE DESIGN DEFINITION AND JUSTIFICATION

To achieve the cross-validation and the image dataset several hardware elements were involved. The following list gives an overview of these elements in detail:

4.1. Air bearing platforms

Three different air bearing platforms have been used at the ORBIT facility which cover three orders of magnitude in terms of mass and inertia:

- ROOTLESS, is lightweight robotic air bearing platforms. The mass of the system without mock-up is 2.95 kg and the inertia is 0.059 kg/m²
- MANTIS, is a medium air bearing platform with a “dry-mass” without air and mock-up of 27.55 kg and an inertia of 1.667 kg/m².
- ACROBAT is the heaviest air bearing platform at ORBIT with a mass of 128.5 kg and an inertia of 8.15 kg/m².

4.2. Position and Motion tracking system

These systems together with the telemetries of the robotic arms, allowed to record the dynamic during and after the contact.

A FARO laser tracker mechanism has been used at GMV for the calibration of the facility at the beginning of every experiment to reproduce the ORBIT reference scenario.

The VICON motion tracking system has been used in ORBIT during the experiments to record the air-bearings position and attitude.

4.3. Load cell

The load cell adopted to measure the contact force/torques is the FTN-GAMMA-2-NETB-0.2 (Calibration SI-130-10) from ROBOTNIK.



Figure 6: Load cell

The load cell measurements were used both to record forces and torques occurred during the contact scenarios and also to close the loop at the *platform-art* facility and to move the KUKA robotic arm according to the contact forces. In this case also the dynamic model was involved to make the KUKA react as if it was the selected air-bearing platform.

4.4. Compliance device

The compliance device is a spring based device with a controlled deformation that can be expressed with a linear law. Its purpose is to include a low stiffness element in the loop, so that this is the only element with non-negligible deformation. Furthermore, thanks to the linear relation between the applied force and the spring deformation, it is possible to simulate the dynamic of the system during and after the contact with the mathematical model that has been developed for the cross-validation. The spring constant has been designed to have deformations of the order of millimeters considering the expected order of magnitude of the contact force, then validated through calibration using the load cell. This device works as a low stiffness component only along its longitudinal axis and it will be used for the simple contact tests.

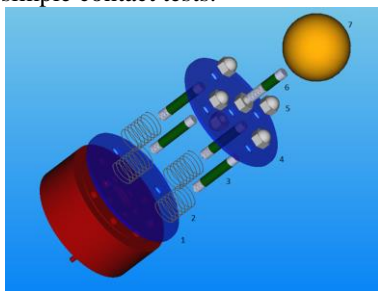


Figure 7: Compliance device

Four springs to store the mechanical energy of the impact. The available sets of spring constants for these experiments are $k=1.5$ N/mm, $k=1$ N/mm, $k=0.3$ N/mm.

4.5. Gripping device

A basic gripping device has been used for such experiments, composed by a MG995 Gripper and a TowerPro MG995 RC Servo commanded by an Arduino based servo control box.

4.6. Mock-ups

Two different mock-ups have been used according to the type of experiment, 3 DOF or 6DOF. The first mock-up is a modular one which was used for the 3 DOF test cases.

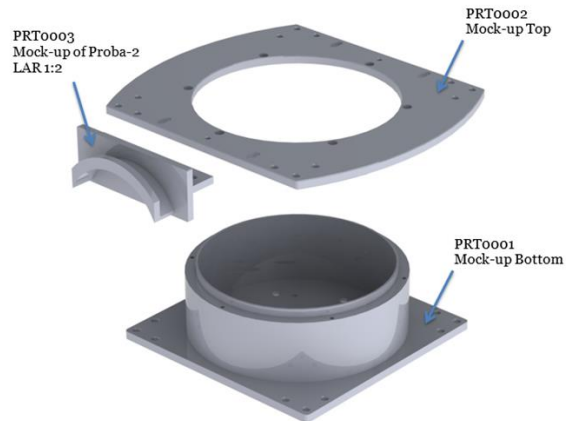


Figure 8: 3 DOF Mock-up

The cylindrical part of the Mock-up (PRT0001) were used as the impacting point for the contact test. The top parts (PRT0002 and PRT0003) includes a Proba-2 like LAR and was used for a gripping scenario during the 3 DOF tests.

Figure 9 shows the satellite mock-up of the 6 DOF experiments. This TANGO mock-up (satellite of the PRISMA Swedish mission from OHB) has been updated with new feature like additional MLI-like covering and 3D printed parts.

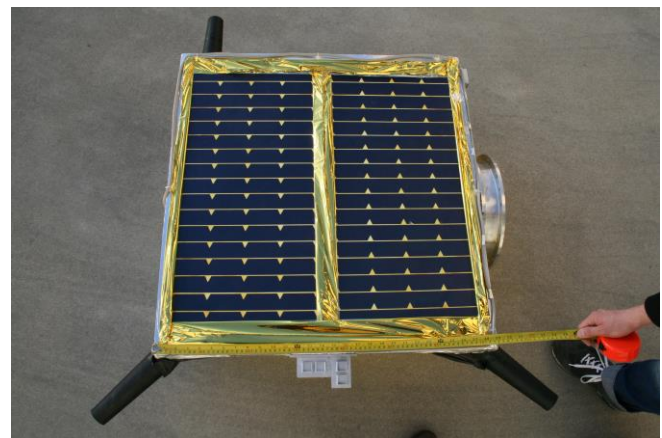


Figure 9: 6 DOF Mock-up (TANGO)

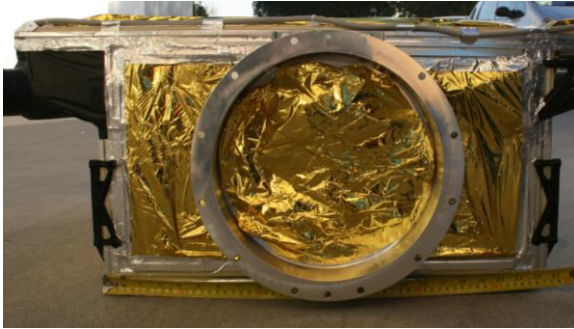


Figure 10: 6 DOF Mock-up (TANGO and LAR)

Furthermore, a PROBA2-like Launch Adapter Ring (LAR) has been manufactured in the laboratory at ESTEC and has been added at the bottom of the mock-up. That part has been used for the gripping at the end of the open loop sequence of the 6 DOF test.

4.7. Cameras

The camera MANTA G-419 was placed near the base of the Mitsubishi robotic arm. This camera has been used in previous activities between ESA and GMV (projects like iGNC and NEO-GNC2-IP) to take pictures for image processing activities. Its characteristics make it a high level space representative camera. On the camera a TECHSPEC COMPACT FIXED FOCAL LENGTH LENS has been mounted (16 mm of focal length) with a FoV of 20 degrees (40 degrees full FoV).

Additionally, a uEye camera was used at the tip of the robotic arm. These cameras provided a sequence of images adopted for the visual confirmation of the success of the gripping sequence.

5. TEST DEFINITION

This section reports the sequence of tests that has been performed. For reasons of clarity, the nomenclature adopted to define a test was chosen in order to include its major characteristics. The adopted code was the following

XXX-NDOF-YYY-(AAA)-MMM-Z

Where:

- **XXX** indicates if the test was performed in the platform-art facility or in the ORBIT facility (respectively PLT and ORB);
- **NDOF** indicates if it refers to a three degree of freedom test or a six degree of freedom test (respectively 3DOF and 6DOF);
- **YYY** indicates if it refers to a simple contact test scenario or a gripping scenario (respectively SCT and GRI);
- **(AAA)** is an optional code that was used only for the PLT-6DOF-GRI group of tests. It indicates the

visual disturbance simulated in the sequence of images taken during the test:

- *FOL* indicates the test in which the fuel on lens disturbance was recreated. This has been done by adding a few water sparks on the lens.
- *MLI* indicates the test in which micro pieces of *MLI* float nearby the target. This has been recreated by dropping pieces of a *MLI*-like foil in the FoV of the camera.
- *PLU* indicates the test in which thruster plume is visible. This effect has been recreated by spraying into the FoV of the camera.
- *IL1* indicates the test in which good illumination conditions are considered as far as the Sun incidence angle is concerned;
- *IL2* indicates the test with the worst case illumination conditions as far as the Sun incidence angle is concerned (limit of working conditions for the reference image processing algorithm);
- *IL3* indicates the test with the source of light in the camera FoV.
- *IL4* indicates the test in which the light direction is chosen to recreate the effect of the *MLI* reflection of the Sun light;
- **MMM** is the ID number of the test;
- **Z** is the code that will be used to indicate the target of the scenario recreated in the test. It will be equal to A if the Mantis air bearing will be adopted (or simulated in platform-art), equal to B if the Acrobat air bearing device will be adopted (or simulated in platform-art), equal to C if the Rootless air bearing device will be adopted (or simulated in platform-art) or equal to D if the mock-up for the 6 DOF tests will be used.

Here below, the list of tests selected for the cross-validation and the database generation is reported together with the nominal relative dynamic characteristics to recreate in the tests. The reported values are the nominal ones: the air-bearing is expected to have similar values but the accuracy is limited by the fact that they are going to depend on the results of manual operations.

TEST	Air bearing angular velocity [deg/s]	Approach velocity of the PA10 [cm/s]
ORB-3DOF-SCT-002-A	0	3

TEST	Air bearing angular velocity [deg/s]	Approach velocity of the PA10 [cm/s]
ORB-3DOF-SCT-003-A	0	5
ORB-3DOF-SCT-004-A	0	10
ORB-3DOF-SCT-007-B	0	5
ORB-3DOF-SCT-008-B	0	10
ORB-3DOF-SCT-009-C	0	1
ORB-3DOF-SCT-010-C	0	3
ORB-3DOF-SCT-011-C	0	5
ORB-3DOF-SCT-012-C	0	10
PLT-3DOF-SCT-020-A	0	1
PLT-3DOF-SCT-021-A	0	3
PLT-3DOF-SCT-022-A	0	5
PLT-3DOF-SCT-028-C	0	1
PLT-3DOF-SCT-029-C	0	3
PLT-3DOF-SCT-030-C	0	5
PLT-6DOF-GRI-FOL-039-D	n.a.	3
PLT-6DOF-GRI-MLI-040-D	n.a.	3
PLT-6DOF-GRI-PLU-041-D	n.a.	3
PLT-6DOF-GRI-IL1-042-D	n.a.	3
PLT-6DOF-GRI-IL2-043-D	n.a.	3
PLT-6DOF-GRI-IL3-044-D	n.a.	3
PLT-6DOF-GRI-IL4-045-D	n.a.	3
PLT-6DOF-GRI-FOL-PLU-IL2-046-C	n.a.	3

Table 2: Test plan

6. 3 DOF TESTS RESULTS

Several additional tests have been performed in order to calibrate the two facilities. Table 2 only reports the most significant ones in the frame of the cross validation.

The stability of all the tests performed in the robotic facility (*platform-art*) was investigated before performing the tests according to the criteria described in [3]. The compliance device has nominally no damping, still a damping factor has been estimated according to the

experimental results in ORBIT. The negligible impact of the contact force on the target attitude (very small friction between the mock-up and the compliance device) suggested that the “collateral” damping of the compliance device was one of the major factors of energy loss in the experiment during the contact.

The selected tests for the cross-validation are reported in the table below.

ORBIT	PLATFORM
ORB-3DOF-SCT-002-A	PLT-3DOF-SCT-021-A
ORB-3DOF-SCT-003-A	PLT-3DOF-SCT-022-A
ORB-3DOF-SCT-010-C	PLT-3DOF-SCT-029-C
ORB-3DOF-SCT-011-C	PLT-3DOF-SCT-030-C

Table 3: Test selected for cross-validation

The communication with the KUKA robotic arm in the *platform-art* setup has a delay of 12 ms. In order to properly reproduce the contact dynamic with the load cell inputs (Hardware-in-the-loop) and the simple contact dynamic models adopted, a no-real time approach has been followed during the tests in the facility. Also real time tests have been executed, but the results are not matching with the ORBIT ones (higher time and force of contact). The reason for this may be because of the simple contact models adopted that only uses the raw data from the load cell. In a context of short contact time (less than 1 s) the 12 ms delay strongly affects the contact dynamic.

6.1. ORB-3DOF-SCT-002-A and PLT-3DOF-SCT-021-A
 In these tests the Mantis (mass of 30 kg) air-bearing platform was adopted, with a linear velocity of the PA10 of 3 cm/s.

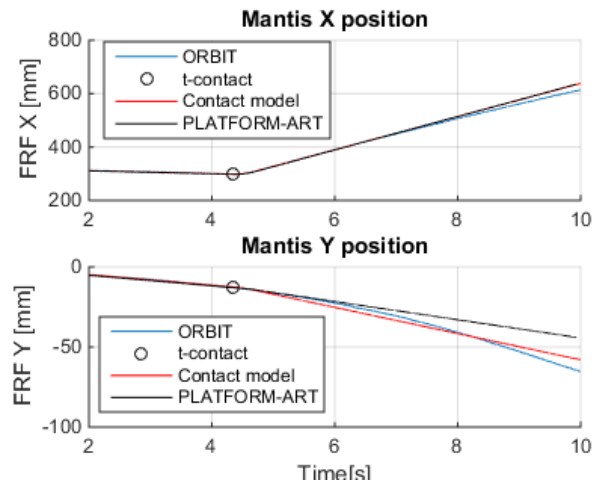


Figure 11: Trajectory of the tests 002 and 021

The dynamic evolution during and after the contact as far as the position is concerned is very similar both in the facilities and considering the contact models results (less than 10% divergence in the X-FRF axis).

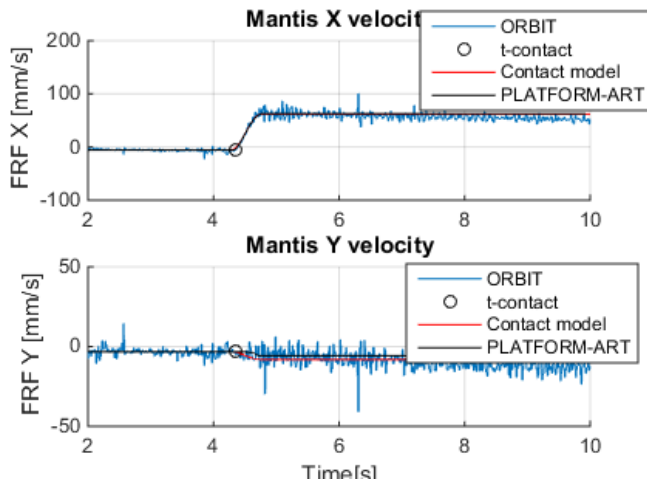


Figure 12: Velocity of the tests 002 and 021

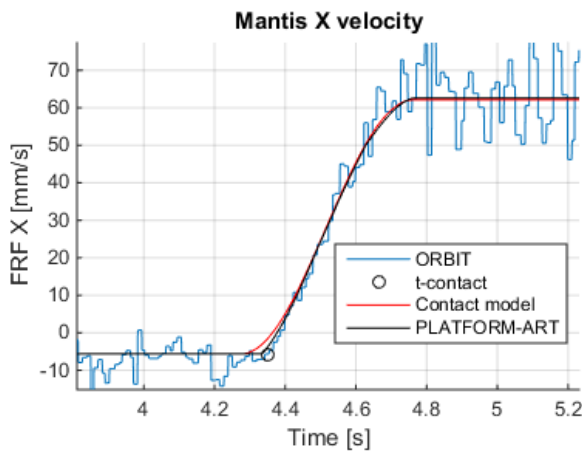


Figure 13: Velocity of the tests 002 and 021 along X-FRF

Also the velocity comparison shows a very good matching (less than 5% relative error just after the contact). It is important to remark that the velocity measured in the ORBIT facility is noisy because it is obtained by deriving the position measurements given by the Vicon system.

In order to fully characterize the contact, also the contact forces along the longitudinal axis measured by the load cell are reported below.

A good matching between the two experimental results and the simulation one is clearly visible in Figure 14, as far as contact duration and force magnitude are concerned.

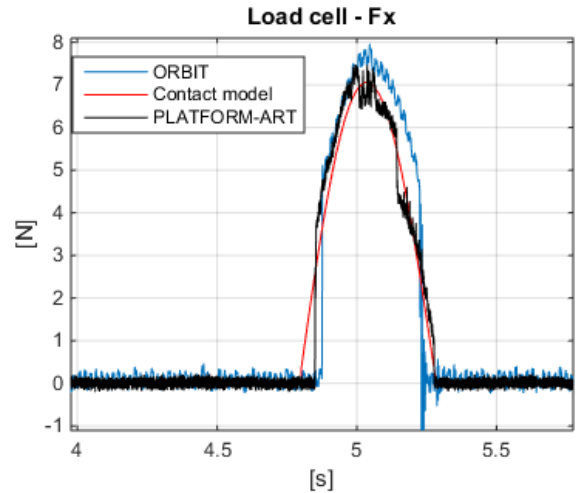


Figure 14: Load cell forces of the tests 002 and 021

6.2. ORB-3DOF-SCT-003-A and PLT-3DOF-SCT-022-A
In these tests the Mantis air-bearing platform was used and approached with a linear velocity of the PA10 of 5 cm/s.

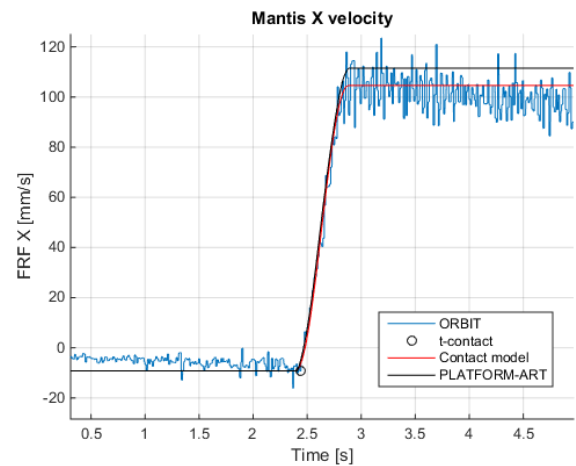


Figure 15: Velocity of the tests 003 and 022 along X-FRF

In this higher velocity tests the matching between the results of the facility is still pretty good. For almost 10 seconds after the contact the difference in velocity considering the results obtained in the two facility is less than 10% of the absolute value (similar behavior of the previous comparison).

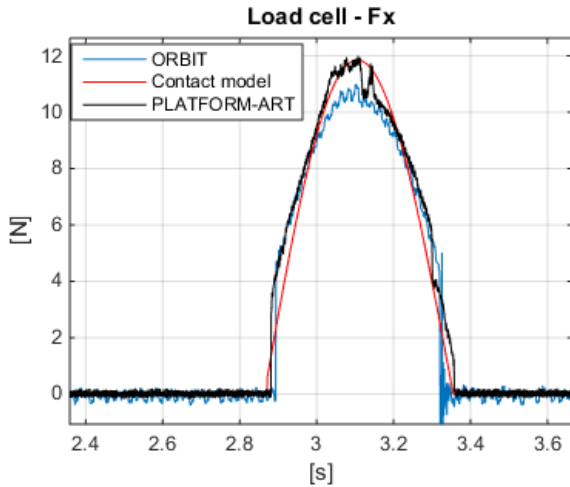


Figure 16: Load cell forces of the tests 003 and 022

Also the contact forces are similar and almost overlapping with the one obtained by simulation results.

6.3. ORB-3DOF-SCT-010-C and PLT-3DOF-SCT-029-C

In these tests the Rootless air-bearing platform was used and approached with a linear velocity of the PA10 of 3 cm/s.

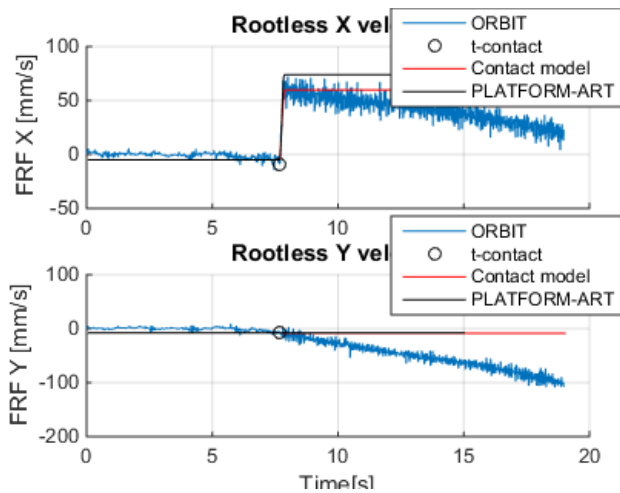


Figure 17: Velocity of the tests 010 and 029

It is possible to notice from Figure 17 that with a lower mass platform the dynamic evolution in the two laboratory is slightly different from the moment of contact. In particular, after the contact there is a quick divergence. This is due to an acceleration in the Y-FRF direction of the Rootless platform that seems to be more sensitive to variations of the floor flatness compared to Mantis.

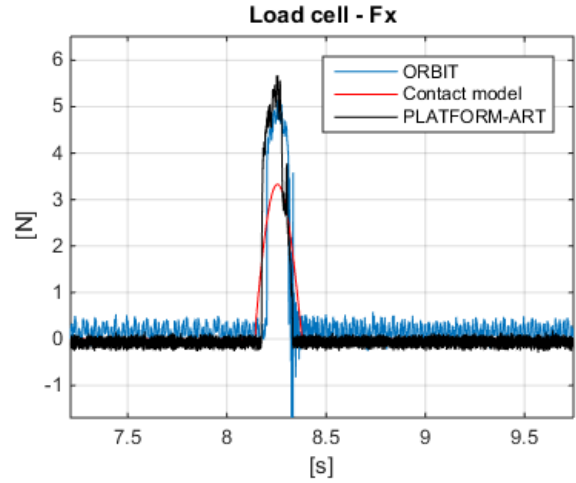


Figure 18: Load cell forces of the tests 010 and 029

From Figure 18 it is possible to appreciate that the contact forces recorded during the experiments in the two facilities are similar between each other, but different from the simulation results. This means that the cross-validation is still valid, but in the low-mass scenario the structural imperfections of the compliance device are not negligible and lead to a mismatch with the simulation results.

6.4. ORB-3DOF-SCT-011-C and PLT-3DOF-SCT-030-C

In these tests the Rootless air-bearing platform was adopted, with a linear velocity of the PA10 of 5 cm/s.

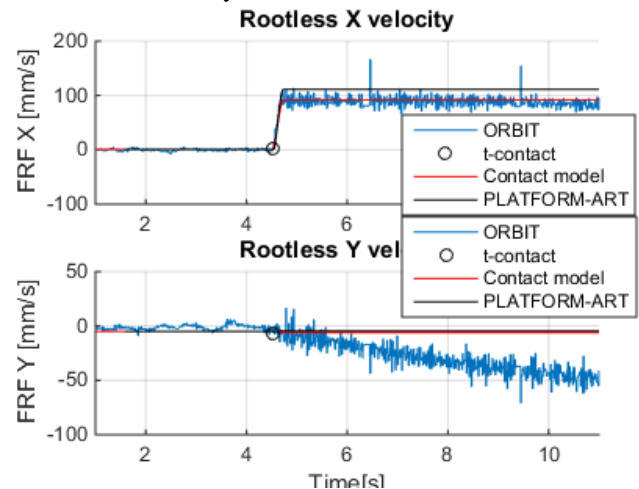


Figure 19: Velocity of the tests 011 and 030

The deviation in the Y-FRF direction of Rootless is still evident. However, if in the low mass scenario the approach velocity is higher (5 cm/s), it is possible to see that the matching between experimental results and simulation ones improves.

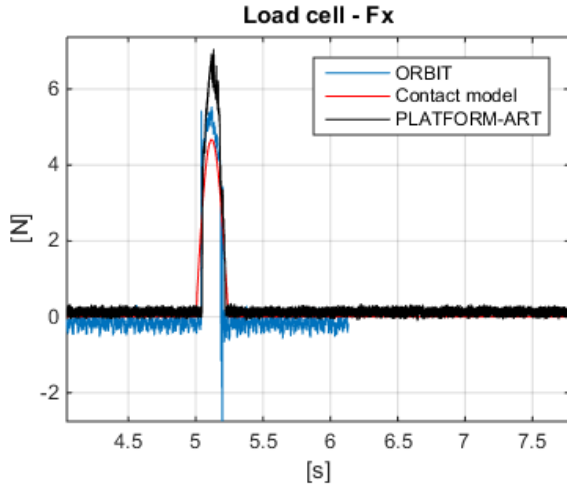


Figure 20: Load cell forces of the tests 011 and 030

Indeed, the contact forces are higher and the compliance device structural imperfections are less significant, even if not negligible (almost 30 % error between contact models and *platform-art* test data).

7. 6 DOF TESTS RESULTS

The 6 DOF tests gave a valuable database of pictures taken by a space representative camera in space-like illumination conditions. Several disturbances and effects have been reproduced in the *platform-art* facility and in this article a few of the pictures of the database are reported. Figure 21 is taken from the good illumination test case, with no disturbances generation during the test. This can be considered the ideal case.

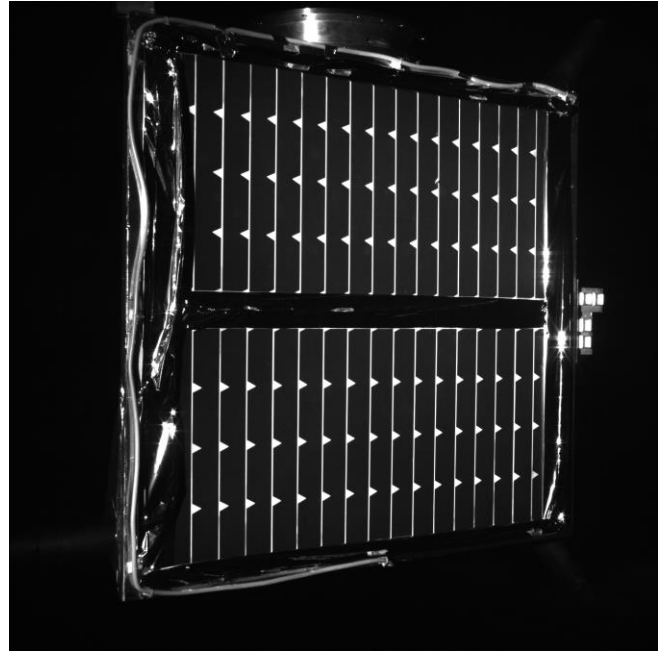


Figure 21: from PLT-6DOF-GRI-IL1-042-D

Figure 22 shows the good illumination case with the MLI floating. As it can be seen from the picture, few pixels are over illuminated.

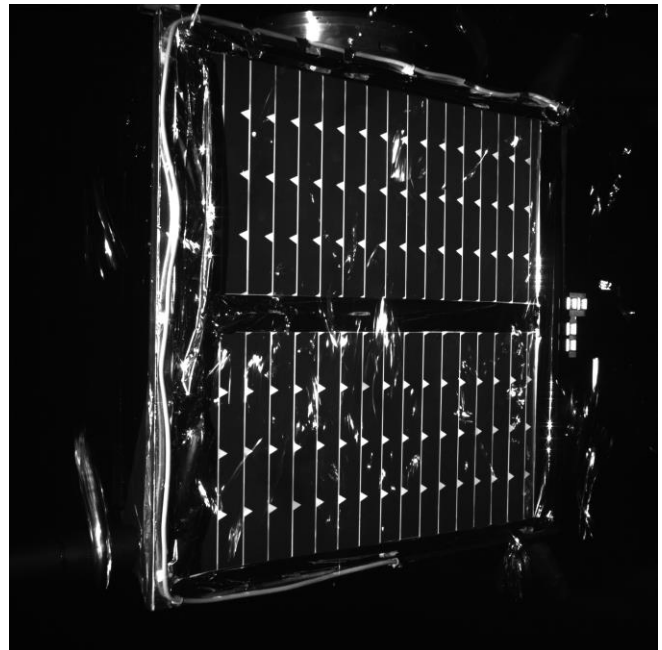


Figure 22: from PLT-6DOF-GRI-MLI-040-D

Figure 23 is taken from the case with the fuel on lens disturbance. Huge areas of the pictures are defocused.

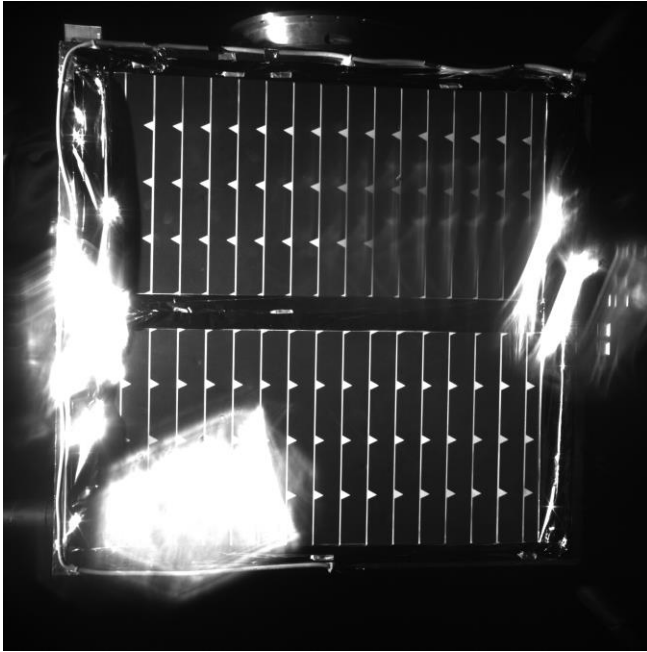


Figure 23: from PLT-6DOF-GRI-FOL-039-D

In Figure 24 the phase angle is very small, so that the MLI reflection is maximized.

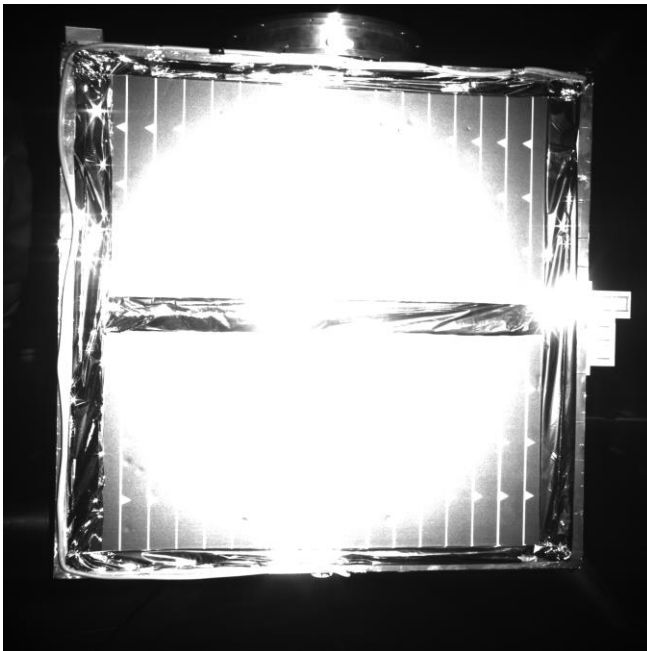


Figure 24: from PLT-6DOF-GRI-IL4-045-D

Figure 25 is taken from the set of images with the thrusters plume in the Field of View. The effect of this disturbance can be considered as a temporary over exposure of the pictures.

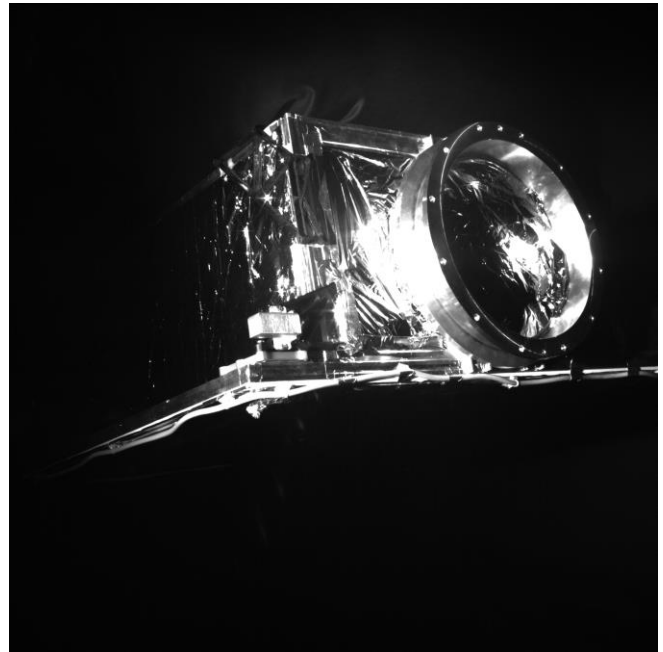


Figure 25: from PLT-6DOF-GRI-PLU-041-D

Figure 26 is taken from the tip camera during the ideal case at the moment of the gripping with the LAR.

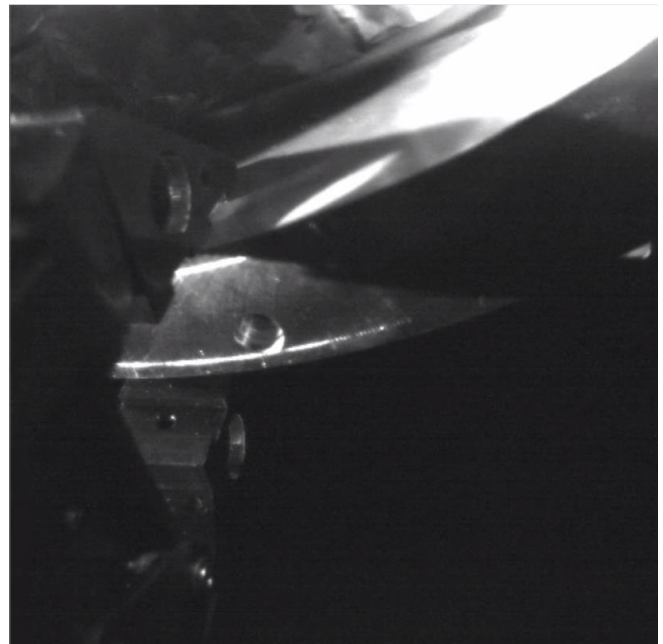


Figure 26: from PLT-6DOF-GRI-IL1-042-D (tip camera)

8. CONCLUSIONS

In the frame of these activity several tests have been performed to cross-validate the capability of ORBIT and *platform-art* to reproduce realistic contact dynamics. In particular, the dynamic regimes in which the facilities can operate has been assessed.

ORBIT operates with real contact and can be considered ground truth for contact forces. The experiments showed that *platform-art* could accurately reproduce the forces when the relative sampling speed of the force sensor is increased by slowing down the simulation respective to real-time. This is mainly due to the 12 ms communication delay with KUKA robotic arm in the current *platform-art* configuration. Also, for safety reasons, only approach velocities smaller than 5 cm/s have been tested.

However, items under test in ORBIT are also subject to small residual external forces after the initial impact. These are mainly due to gravity and the non-perfect flatness of the floor as well as friction. This limits the accuracy of trajectories as they evolve over time. The tests performed, showed that in the case of low mass, inertia and velocity such influences are the most pronounced. In the particular case of the low mass platform (Rootless) and linear approach at 3 cm/s, the trajectory and the post-impact velocity were accurate to within 10 % with respect to the nominal value for 1.5 seconds after the contact.

Errors in the trajectory simulated with *platform-art* after initial impact are mainly due to errors in the initial conditions, namely the aforementioned difficulty of measuring the contact forces.

As a consequence of these measurements, it can be said that low stiffness and high damping values should be considered as a general design rule for the compliance device for reasons of stability of the closed-loop control in *platform-art*.

Furthermore, low masses of the order of a few kilos should be avoided since they can, especially at higher speeds, introduce instability in the controller of *platform-art*.

The study demonstrated that *platform-art* is a powerful tool to simulate contact dynamics so long as care is taken to ensure that these conditions are met.

It also showed that flat floors facilities are limited in the free drift phase (after impact) due to the non-perfect flatness of the floor, but that an accurate trajectory can be obtained by carefully limiting the duration of the experiment and the mass and velocity of the platform.

The activity also remarked the *platform-art* capability of re-creating a space-like scenario in terms of illuminations and disturbances reproduction. The database of images has been generated and it is ready to be used to test the robustness of image processing algorithms.

9. REFERENCES

- [1] H. Kolvenbach, K. Wormnes, "ORBIT – A Facility for Experiments on Free Floating Contact Dynamics", 13th Symposium on Advanced Space Technologies in Robotics and Automation (ASTRA), 2015.
- [2] P. Colmenarejo, E. di Sotto and J. A. Bejar "Dynamic test facilities as ultimate ground validation step for space robotics and GNC system", 6th ICATT, 2016.
- [3] M. Zebany, R. Lampariello, T. Boge and D. Choukroun, "A new contact dynamics model tool for hardware-in-the-loop docking simulation", 11th International Symposium on Artificial Intelligence, Robotics and Automation in Space (i-SAIRAS), 2012.